Chemical Science International Journal

24(4): 1-10, 2018; Article no.CSIJ.43904
ISSN: 2456-706X
(Past name: American Chemical Science Journal, Past ISSN: 2249-0205)

Analysis of Pure and Ag-Doped TiO_2 Thin Films Deposited by Field Assisted Spray Pyrolysis

Arishi, Jennifer Ifeoma[1*] and Ozuomba, Jude[1]

[1]Department of Physics, Imo State University, Owerri, Nigeria.

Authors' Contributions

This work was carried out in collaboration between both authors. Authors AJI and OJ designed the research. Author AJI performed the experiment, data collection and analysis. The first draft of the manuscript was written by author AJI. Author OJ managed the second draft. Both authors read and approved the final manuscript.

Article Information

DOI: 10.9734/CSJI/2018/43904
Editor(s):
(1) Dr. Francisco Marquez-Linares, Department of Chemistry, Nanomaterials Research Group, School of Science and Technology, University of Turabo, USA.
Reviewers:
(1) Hermes José Loschi, University of Campinas (UNICAMP), Brazil.
(2) Anukorn Phuruangrat, Prince of Songkla University, Thailand.
(3) Joel Obed Herrera Robles, Autonomous University of Ciudad Juarez, Mexico.
Complete Peer review History: http://www.sciencedomain.org/review-history/27143

Original Research Article

Received 02 July 2018
Accepted 09 September 2018
Published 10 November 2018

ABSTRACT

This paper reports the structural and optical properties of Undoped TiO_2 and 5% Ag-doped TiO_2 nanoparticles under visible- light irradiation. These films were synthesised using Electrohydrodynamic Spray Pyrolysis Technique, deposited at 250°C and later annealed at 400°C few minutes. The films were characterised by Surface Profilnometry, Ultraviolet – Visible light Spectroscopy (UV-Vis Spectroscopy), Optical Microscope and X-ray diffraction (XRD). The result from surface profilometry showed that the thickness of all the samples is thin films. XRD results showed that all the films have crystalline nature of TiO_2 and annealed films result in an increase of crystallinity. The crystal phase observed was trigonal for both TiO_2 and 5% Ag doped TiO_2. The unannealed Undoped TiO_2 exhibited low absorbance within the visible spectrum but increases as we dope with 5% Ag-doped TiO_2 and effect of annealing increases the absorbance. Extinction coefficient increases within the visible region as we doped and thermal annealing also increases its effect within the visible region. The study of the microstructural properties using Optical Microscopy showed an increase in the hardness of the film for annealed films and they have micro-grains that

**Corresponding author: E-mail: epheoma1@gmail.com;*

are closely packed compared to unannealed samples. The direct band-gap for unannealed films range from 4.70 eV- 3.10 eV while annealed films was between 3.20 eV and 2.80 eV. Doped Annealed films showed reduced band-gap.

Keywords: Ag doped TiO_2; field assisted spray pyrolysis; structural properties; optical properties and wide band gap semiconductor.

1. INTRODUCTION

Titanium dioxide (TiO_2) also known as titania is the most promising electron acceptor and a very useful wide band-gap semiconducting transition metal oxide which has attracted much interest among researchers due to its unique characteristics such as non-toxicity, affordability, easy handling, resistance to photochemical and chemical erosion [1]. It is a wide band-gap semiconductor with energy of 3.0–3.4 eV and is widely used in applications such as hydrogen production [2], gas sensor [3,4], photo catalytic activities [5], dye-sensitised solar cells and photo electrochemical cells because of its relative high efficiency and high stability. TiO_2 exists in both crystalline and amorphous forms. In Its existence in three crystalline polymorphs, namely, anatase, rutile and brookite, anatase and rutile have a tetragonal structure, whereas brookite has an orthorhombic structure [6].

There are different routes that can be used to synthesise titanium dioxide. These include a conventional solid state route [7,8], precipitation [9,10], Sonochemical [8], hydrothermal [11,12], microwave hydrothermal [13] and sol-gel methods [14,15]. Titanium dioxide (TiO_2) also exhibits useful electrical, optical, and photocatalytic behaviour due to the powerful oxidation and reduction properties that arise in the absorption of photon energy [16].

Due to TiO_2 wide band–gap which ranges from 3.0eV- 3.4eV, between the valence and conduction bands, there is a significant limitation with regards to the photocatalytic applications. Hence several attempts have been made by researchers to improve its absorbance within the visible region thus enhancing its photocatalytic activities through the process of doping [17].

In this work, we carried out a comparative analysis of the different deposited samples to identify the effect of concentration of dopant and the effect of thermal annealing on the samples using Electrohydrodynamic Spray Pyrolysis Technique. The films deposited were characterised by Surface Profilnometry, Ultraviolet – Visible light Spectroscopy (UV-Vis Spectroscopy), Optical Microscopy and X-ray diffraction (XRD).

2. EXPERIMENTAL

TiO_2 was synthesised using 0.2 mol of titanium acetyl acetonate [$Ti(C_5H_7O_2)_4$] and 20 mol of propanol [C_3H_8O] as the precursor while 0.68 g of silver nitrate [$AgNO_3$], mixed with 20 mol of propanol in a conical flask, placed on a magnetic stirrer and was stirred with the magnetic stirring bar, until the $AgNO_3$ was properly dissolved served as the precursor for Silver(Ag). The precursor delivery system containing string pump was formatted using a laptop to get accurate atomization or deposition. The flow rate was set at 4200microlitres/ hour, the volume was set at 400microlitres/hour and the time of deposition was set at 10mins. The Electrohydrodynamic Spray Pyrolysis Techique was set at the voltage of 3.5KV and the distance between the nozzle and the substrate (pro cleaned glass) was 5.95mm. From the precursors we obtained

$$4AgNO_3 + Ti(C_5H_7C_2)_4 = 4(Ag(C_5H_7O_2)) + Ti(NO_3)_4$$

5% Ag doped TiO_2 was deposited at 250°C and was duplicated to get two samples. Undoped TiO_2 was also deposited at 250°C and also duplicated to two samples. Hence we have a total of four (4) samples. One 5% Ag doped TiO_2 and one undoped TiO_2 were later annealed at 400°C in few minutes using master chef annealing machine with Model No: P70BI7L-Ds(7014336), in order to expel the water of crystallisation from the samples.

The thickness of the synthesised samples (both doped and undoped) was measured using surface profilenometry with a VeecoDektak 150 profiler machine. Using UV-Vis spectroscopy, the absorption spectra of the deposited undoped TiO_2 and Ag- doped TiO_2 thin films were recorded within the wavelength range of (UV) region of (230 nm to 390 nm), visible light (VIS) region of (400 nm to 700 nm) and near infrared

(NIR) region of (714 nm to 1080 nm). The reflectance values of the work were obtained using a relation between the absorbance (A), transmittance (T) and reflectance (R), according to the law of conservation of energy given by

$$A + T + R = 1 \quad (1.1)$$

From equation 1.1, reflectance (R) was given as

$$R = 1 - T - A \quad (1.2)$$

The values of refractive index of were obtained using the equation of refractive index according to (Ali et al., 2015),

$$\eta = (1 + \sqrt{R}) / (1 - \sqrt{R}) \quad (1.3)$$

Where R is the reflectance and η is the refractive index.

The values of extinction coefficient of this work were calculated using the equation of extinction coefficient according to[18]

$$K = \alpha\lambda/4\pi \quad (1.4)$$

Where k is called the extinction coefficient (k), α is the absorption coefficient, λ is the wavelength, π is equal to 3.142.

The microstructural properties of both doped and undoped TiO_2 were determined using Light Microscope; Celestron LCD digital microscope. (Model no: 44348), under the magnification of 800. The XRD pattern was recorded on a Rigaku Ultima IV X-ray diffractometer equipped with a graphite- monochromated Cu Kα radiation source (40kv, 30mA) and wave length 1.54Å. A diffractogram was collected in the 2θ range between 3° and 90° with a step size of 0.01° and a scan speed of 1^0/min. the XRD Pattern was processed using JCPDS card numbers. We used Debye Scherer equation to calculate for the crystallite size.

$$D = k\lambda / \beta\cos\theta \quad (1.5)$$

Where D is the crystallite size, K= shape factor, which is constant (0.89), λ = wavelength (1.54Å), β = Full Width Half Maximium (FWHM), θ= 2 Theta, which to obtain θ, we divided by 2.

3. RESULTS AND DISCUSSION

The thickness of the synthesised samples (both doped and undoped) was measured using surface profilometry with a VeecoDektak 150 profiler machine; the result showed that all the samples are thin films.

3.1 Optical Properties of the Deposited Films

The absorbance spectra of the deposited films were shown in Fig. 1a and 1b. It is found that absorbance spectra of 5% Ag doped TiO_2 has high absorbance within the visible region than the undoped TiO_2. Comparing the annealed and unannealed films, it also showed that annealed films have the best absorbance within the visible region than unannealed films.

Figs. 2a and 2b below showed the extinction coefficient of unannealed samples and annealed samples. It showed that doping increases the extinction coefficient of the film within the visible region.

using Tauc's relation

$$\alpha h\nu = A(h\nu - E_g)^n \quad (1.6)$$

where hv is the photon energy, h is Planck's constant, α is the absorption Coefficient, A is the constant, for direct transitions n=2, and E_g is the optical band gap, which is given as

$$E_g = h\nu = hc/\lambda \quad (1.7)$$

C is the velocity of light = 3×10^8 ms^{-1} λ is the wavelength in meters (m). υ Is the transition frequency, h is the Planck's constant = 6.62×10^{-34}Js. Since 1J = 1.602×10^{-19} eV

We substituted these variables into equation 1.7 and obtained

$$h\upsilon(\mathrm{eV}) = \frac{hc}{\lambda_o} = \left(\frac{6.63 \times 10^{-34} Js \times 3 \times 10^8 \mathrm{ms}^{-1}}{\lambda \times 1.602 \times 10^{-19} \mathrm{c}}\right)$$
$$= \left(\frac{6.63 \times 10^{-34} Js^{-1} \times 3 \times 10^8 ms^{-1}}{\lambda(\mathrm{nm}) \times 10^{-9} \times 1.602 \times 10^{-19} \mathrm{c}}\right)$$

$$h\nu \text{ (eV)} = 1.241/\lambda\ (\mu m) \quad (1.8)$$

From equation 1.8 we calculated the photon energies in (eV) for various wavelengths λ in(μm). A graph of $(\alpha h\nu)^2$ versus hv for both unannealed and annealed samples were plotted and the direct band gap was extracted by extrapolating the straight portion of the graph on hυ axis at $(\alpha h\upsilon)^2 = 0$ which gives the band gap of both unannealed and annealed films. For unannealed, the undoped TiO_2 has the band gap of 4.70eV while 5% -doped Ag has band gap of 3.10eV which shows that doping brings about reduction of the energy band gap from the graph Fig 3a.

For the annealed films, the undoped TiO_2 has the band gap of 3.20eV which is in agreement with undoped TiO_2 result obtained by [19] while the 5%-doped Ag has 2.80eV similar to result obtained by [20]. The annealed films have narrowed energy band gap than the unannealed films. see Fig. 3b.

3.2 The Micrograph Analysis

Figs. 4a- 4b show the micrograph of unannealed and annealed samples of TiO_2 using Celestron LCD digital microscope, model #44348 with magnification of 800. Fig. 4a shows the micrograph of undoped unannealed TiO_2 sample

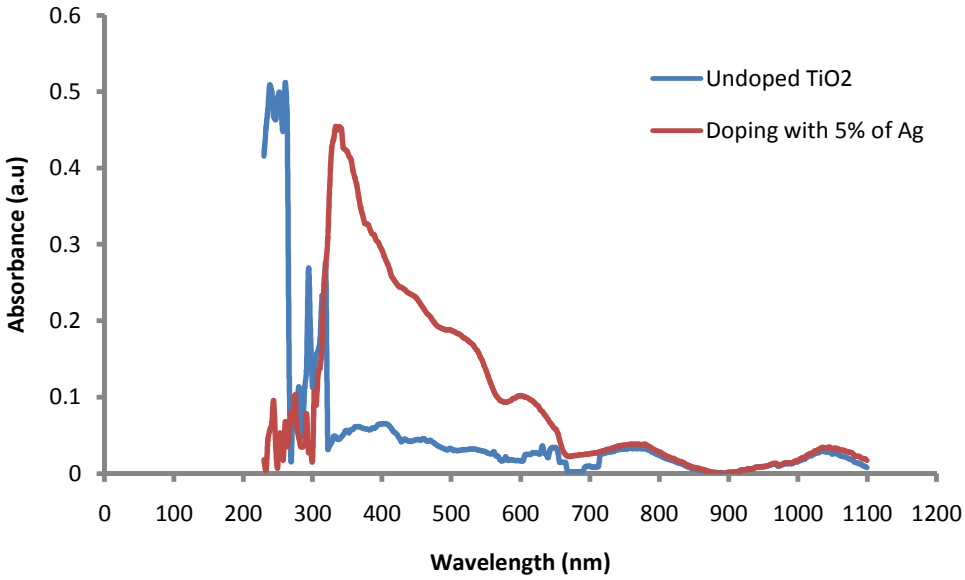

Fig. 1a. Absorbance spectra for the undoped and doped unannealed samples

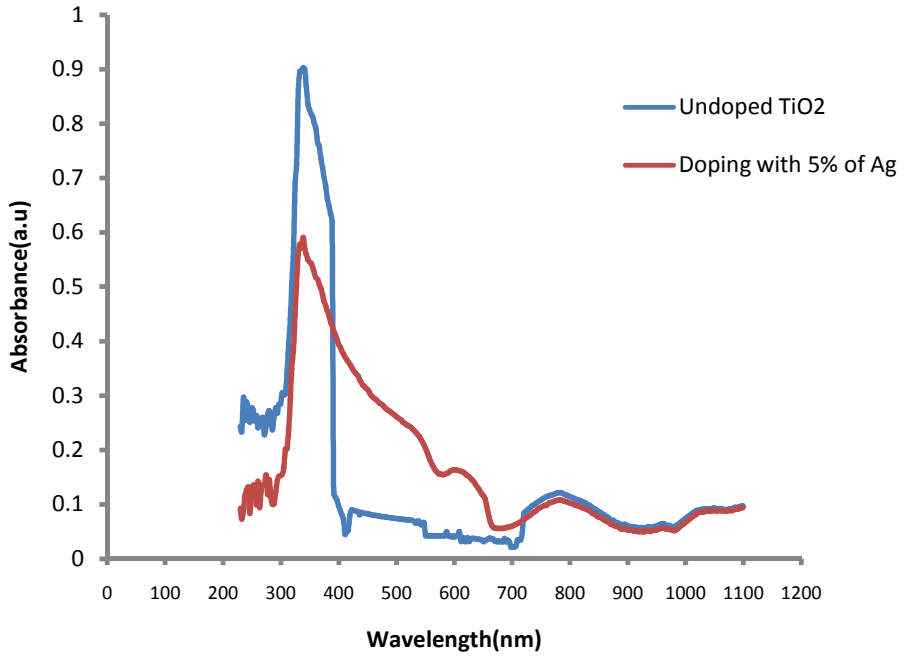

Fig. 1b. Absorbance spectra for the undoped and doped annealed samples

which reviewed rough surface morphologies and larger pores on the film, which may be due to the aggregation of tiny crystals and the time of deposition. Using imageJ app, we obtained an average particle size of 6.00 while Fig. 4b, the micrograph of undoped annealed TiO_2 sample reviewed an increase in the number of orderly stacked grains. There was reduction in the size of pores and there was increase in the hardness of the film compared to unannealed sample. The average particle size of 8.00 was obtained using imageJ app.

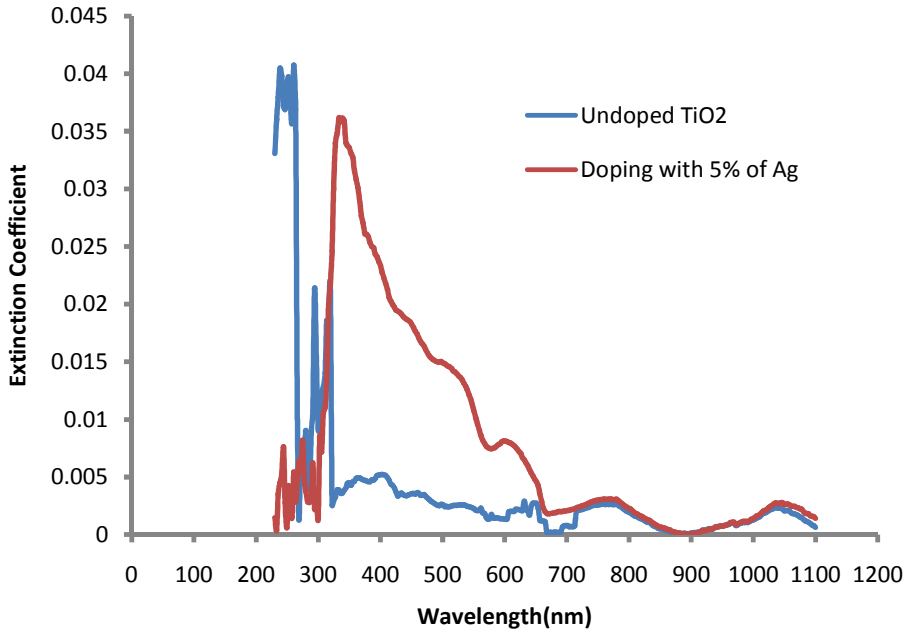

Fig. 2a. Dependence of extinction coefficient on the wavelength for undoped and doped unannealed sample

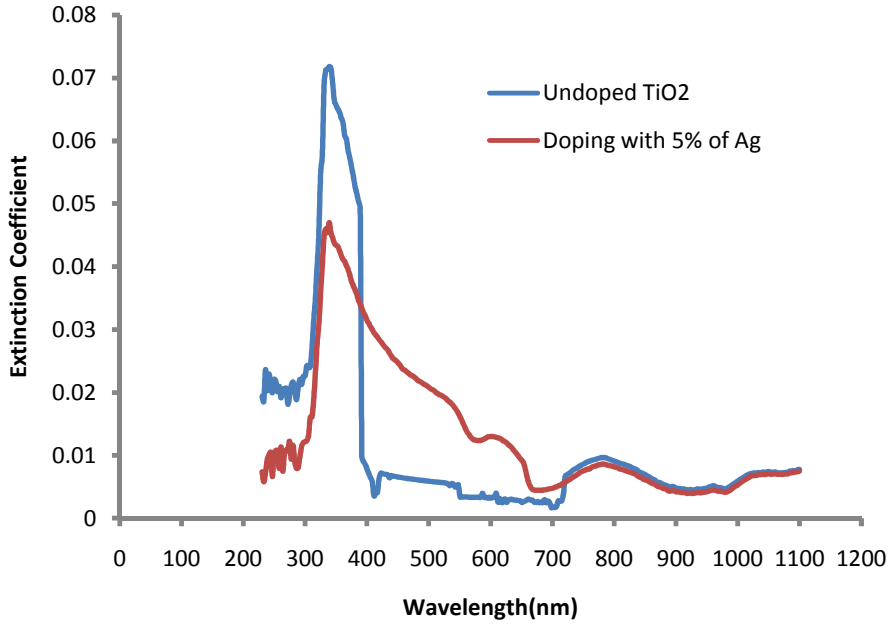

Fig. 2b. Dependence of extinction coefficient on the wavelength for undoped and doped annealed samples

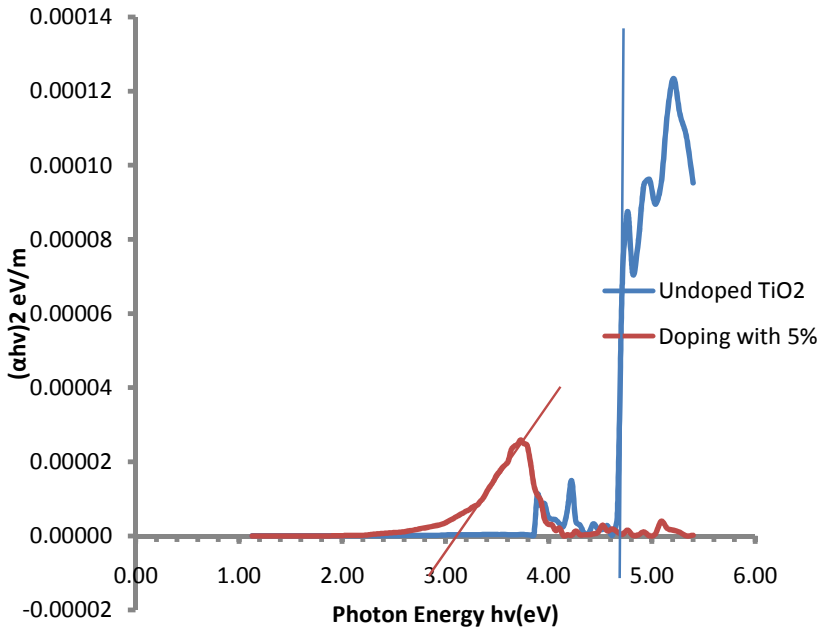

Fig. 3a. Direct band gap for unannealed undoped TiO_2 and 5%-doped Ag films

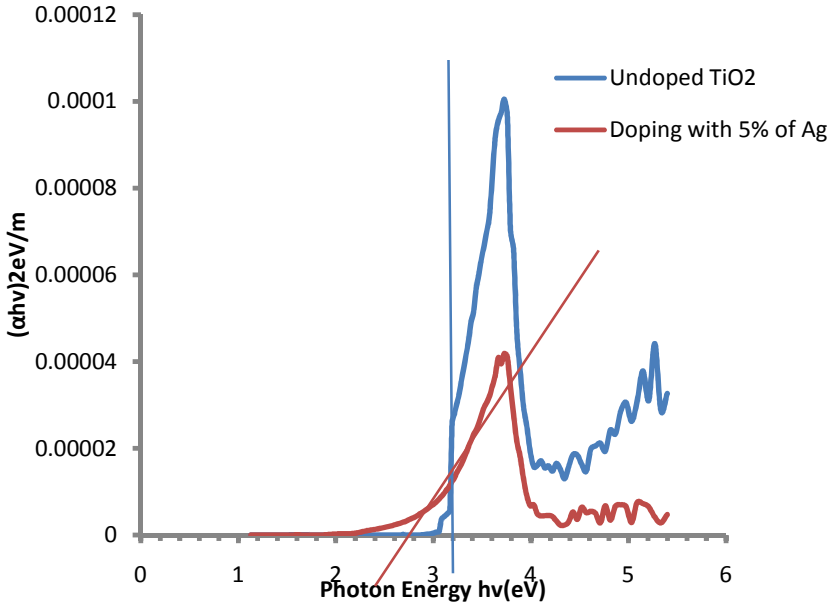

Fig. 3b. Direct band gap for annealed undoped TiO_2 and 5%-doped Ag films

Figs. 5a- 5b show the micrograph of unannealed and annealed samples of 5% of Ag/TiO_2 using Celestron LCD digital microscope, model #44348 with magnification of 800. Fig. 5b shows rough surface morphology of the film; larger pores and larger grains were evident. Using imageJ app, we obtained an average particle size of 7.00 while Fig. 5b shows the micrograph of annealed 5% Ag/TiO_2 sample. Close observation reviewed that micro grains are packed closely compared to unannealed sample. There was increase in the hardness of the film and using imageJ app, we obtained an average particle size of 9.00.

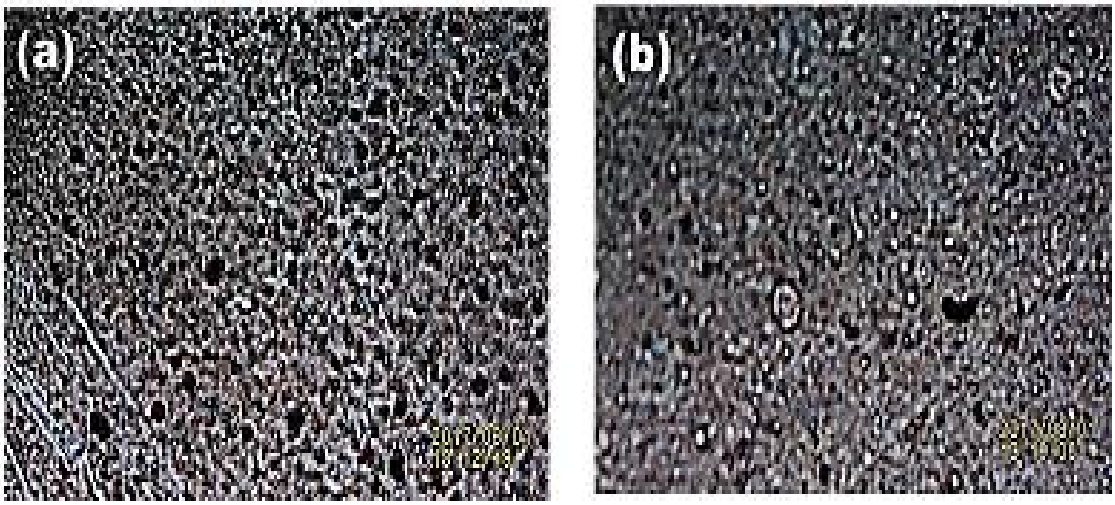

Fig. 4. Micrograph of Undoped TiO_2, (a) unannealed sample (b) annealed sample

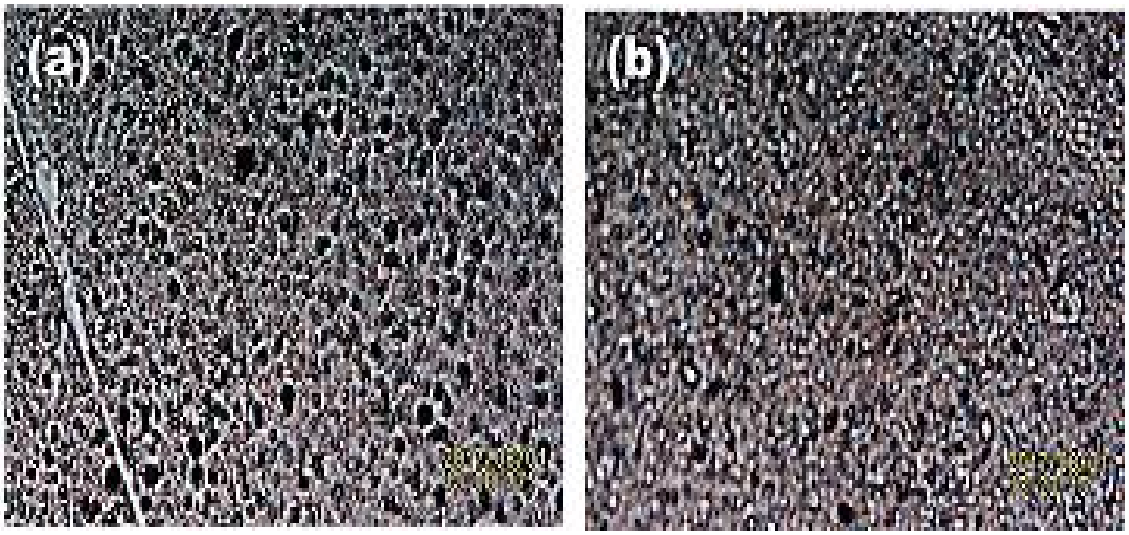

Fig. 5. Micrograph of 5% Ag:TiO_2, (a) unannealed sample (b) annealed sample

3.3 The X-ray Diffraction

Fig. 6 show the x – ray diffraction patterns for both Annealed and Unannealed undoped TiO_2 samples with peaks at 2θ = $25.30°$, $27.56°$, $37.99°$, $48.25°$, $54.22°$, $62.65°$ and $74.80°$ which correspond to miller indices [101], [110], [103], [200], [105], [213] and [107] respectively. These results show that the samples are of trigonal crystalline phase of TiO_2 which correspond to the Crystallography Open Database (COD) entry file number of 96 – 153 – 7225. Using Debye-Scherer equation the average crystallite was 8.78nm and 8.76nm respectively. Comparing the two, the annealed TiO_2 pattern had well defined or high intensity of peaks than the undoped unannealed TiO_2 sample.

Fig. 7 shows the x – ray diffraction patterns for 5% Ag of both annealed and unannealed samples. They have diffraction peaks at 2θ = $25.33°$, $27.49°$, $37.98°$, $48.31°$, $54.28°$, $62.47°$ and $74.89°$ which correspond to miller indices [j101], [110], [103], [200], [105], [213] and [107] respectively. The results show that the Ag doped TiO_2 are crystalline in nature. The x -ray spectra were matched with the standard data using Match3 software. The result corresponds to the Crystallography Open Database (COD) entry file number of 96 – 153 – 7225. There was no

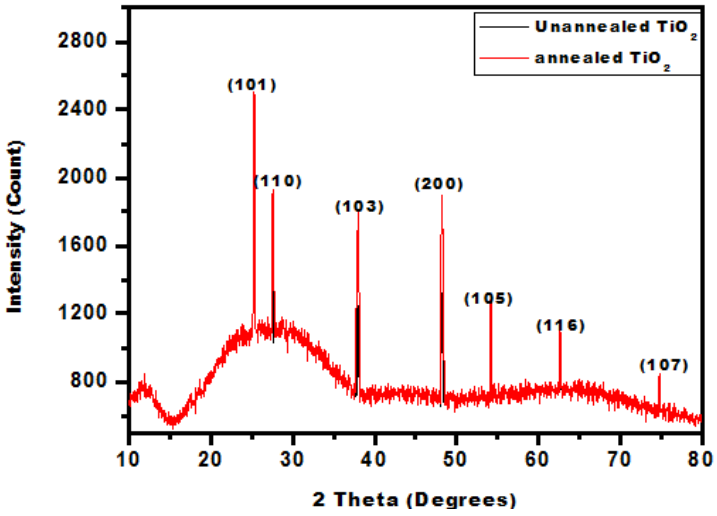

Fig. 6. X- ray Diffraction Pattern for Undoped Unannealed TiO_2 and Undoped Annealed TiO_2

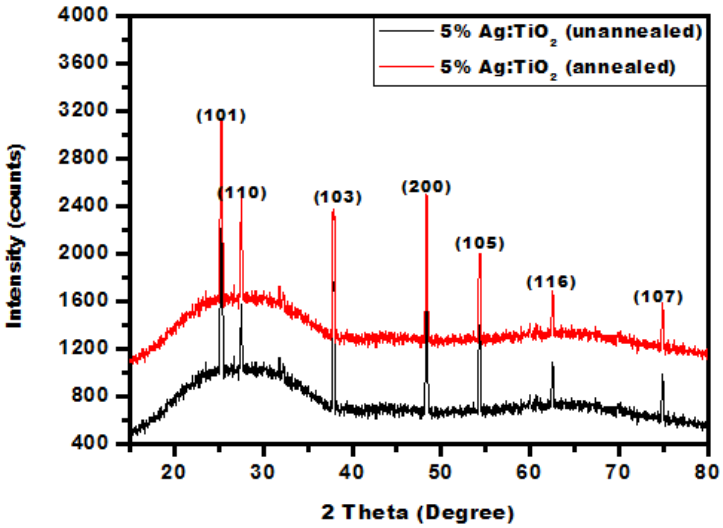

Fig. 7. X- ray diffraction pattern for both 5% of Ag/TiO_2 annealed and unannealed samples

Significant shift in the peak position of diffraction patterns of both annealed and unannealed 5% doped with ag, except the changes in the intensity of these peaks. Annealed sample had well defined or high intensity of peaks than the unannealed sample due to annealing of the sample. Using debye-scherer equation the average crystallite was 8.80nm and 8.76nm respectively.

4. CONCLUSION

In this paper we have reported the structural, optical properties of TiO_2 and Ag-doped TiO_2 synthesised using Electrohydrodynamic spray pyrolysis equipment. The XRD pattern showed crystalline nature of TiO_2. There was increase in the crystallinity of the films in the case of annealed. UV- vis spectroscopy revealed the shifting of absorption edge of silver-doped TiO_2 to the visible region compared to that of Undoped TiO_2 and the annealed films showed higher absorbance than unannealed films. The Extinction coefficient showed that as the dopants are been added to the parent material, the extinction coefficient values of the films increases within the visible region. The direct band gap for annealed showed more decrease in energy band

gap than the unannealed doped samples. Using Optical Microscopy showed increase in the hardness of the film for annealed films and they have micro-grains that are closely packed compared to unannealed samples. For the unannealed, the direct band gap ranges from 4.70eV – 3.10eV and the annealed the direct band gap ranges from 3.20eV – 2.80eV. The undoped TiO_2 nanoparticles showed poor photocatalytic activity, while doping of silver ions improves the efficiency under the visible –light irradiation.

COMPETING INTERESTS

Authors have declared that no competing interests exist.

REFERENCES

1 Hoffmann MR, Martin ST, Choi W, Bahnemann D. Environmental applications of semiconductor photocatalysis. Journal of Chemical Reviews. 1995;95:69-96.

2 Zaleska, A. Characteristics of doped-TiO_2 photocatalys. Journal of Physiocochemical Problems of Mineral Process. 2008;4:211-222.

3 Sayilkan F, Asilturk M, Sayilkan H, Onal Y, Akarsu M. Characterization of TiO_2 synthesized in alcohol by a sol-gel process: Effects of annealing temperature and acid catalyst. Turkisk Journal of Chemistry. 2005;30:697-706.

4 Gomez A, Meghraoui M. Holocene faulting and earth quake recurrence along the Serghaya Branch of the Dead Sea Fault System in Syria and Lebanon. Geophysical Journal International. 2003;21:658-674.

5 Yogeswaran U, Chen SM. Recent trends in the application of carbon nanocubes-polymer composite modified electrodes for biosensors. Journal of Analytical Letters. 2008;2:210-243.

6 Mahshid S, Askari M, Ghamsari MS. Effect of brookite presence on nanocrystalline anatase – rutile phase transformation. International Journal of Nanotechnology. 2007;8:11365-8486. Available:https://doi.org/10.1504/ijnt.2009.027559

7 Dong Hyun Kima HS. Photocatalytic behaviours and structural characterization of nanocrystalline Fe-doped TiO_2 synthesized by mechanical alloying. Journal of Alloys and Compounds. 2004; 375:259–264.

8 Guimarães J, Abbate M, Betim S, Alves M. Preparation and characterization of TiO_2 and V_2O_5 nanoparticles produced by Ball-milling. Journal of Alloys and Compounds. 2003;352:16–20.

9 Joo J, Kwon S, Yu J, Hyeon T. Synthesis of ZnO nanocrystals with cone, hexagonal cone, and rod shapes via non-hydrolytic ester elimination sol–gel reactions. Journal of Advance Materials. 2005;17:1873–1877.

10 Lee JH, Yang YS. Effect of HCl concentration and reaction time on the change in the crystalline state of TiO_2 prepared from aqueous $TiCl_4$ solution by precipitation. Journal of the European Ceramic Society. 2005;25:3573–3578.

11 Hidalgo MC, Moncayo MA, Maicu M, Colón G. Hydrothermal Preparation of highly Photoactive TiO_2 Nanoparticles. Journal of Catalysis Today. 2007;129:50-58.

12 Deshpandea AGM. Role of lattice defects and crystallite morphology in the UV and Visible-light-induced photo-catalytic properties of combustion-prepared TiO_2. Journal of Materials Chemistry and Physics. 2011;126:546–554.

13 Murugan AV, Samuel V, Ravi V. Synthesis of nanocrystalline anatase TiO_2 by microwave hydrothermal method. Journal of Materials Letters. 2006;60:479-480.

14 Pookmanee P, Phanichphant S. Titanium dioxide powder prepared by a sol-gel method. Journal of Ceramic Processing Research. 2009;10:167-170.

15 Tiberiu D, Ligia T, Adriana R, Maria Z. Nanosized Al_2O_3-TiO_2 oxide powder with enhanced porosity obtained by sol-gel method. Journal of Academia Română. 2014;59:125-134.

16 Kim DS, Kwak SY. The hydrothermal synthesis of mesoporous TiO_2 with high crystallinity, thermal stability, large surface area, and enhanced photocatalytic activity. Journal of Applied Catalysis. 2007;323: 110-118.

17 Ambrus Z, Bala´zs N, Alapi T, Wittmann G, Sipos P, Dombi A, Mogyoro K. Synthesis, structure and photocatalytic properties of Fe (III)-doped TiO_2 prepared from $TiCl_3$. Journal of Applied Catalysis. 2008;81:27–37.

18 Mahrov B, Boschloo G, Hyfeldt A, Siegbahn H, Rensmo H. Photoelectron Spectroscopy studies of Ru(dcbpyH2)2(NCS)2/CuI and

Ru(dcbpyH2)2/CuSCN interfaces for solar cell applications. Journal of Physical Chemistry. 2004;108:11604–11610.

19 Hassan MM, Haseeb AS, Saidur H, Masjuki M. Effects of annealing treatment on optical properties of anatase TiO_2 thin films. International Journal of Chemical and Bimolecular Engineering. 2008;1:93-97.

20 Ayieko CO, Musembi RJ, Waita SM, Aduda BO, Jain PK. Structural and optical characterization of nitrogen-doped TiO_2 thin films deposited by spray pyrolysis on fluorine doped tin oxide (FTO) coated glass slides. International Journal of Energy Engineering. 2012;2:67-72. Available:http://dx.10.5923/j.ijee.0203.02

Peer-review history:
The peer review history for this paper can be accessed here:
http://www.sciencedomain.org/review-history/27143